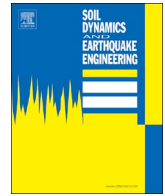




ELSEVIER

Contents lists available at ScienceDirect

Soil Dynamics and Earthquake Engineering

journal homepage: www.elsevier.com/locate/soildyn

Multi-objective loss-based optimization of viscous dampers for seismic retrofitting of irregular structures[☆]

Arun M. Puthanpurayil^a, Oren Lavan^{b,*}, Rajesh P. Dhakal^a

^a Civil & Natural Resources Engineering, University of Canterbury, Christchurch, New Zealand

^b Faculty of Civil and Environmental Engineering, Technion - Israel Institute of Technology, Haifa 32000, Israel

ABSTRACT

In this paper an efficient first-order multi-objective optimization scheme is adopted for the design of linear viscous dampers for the seismic retrofitting of frame buildings. A retrofitting cost function serves as one objective while the expected losses serve as the other objective. These two objectives are well understood by decision makers that may not be engineers. Furthermore, with the Pareto front for these two objectives at hand, the decision maker can make his decisions with the whole picture at hand. To allow achieving the Pareto front with a reasonable computational effort, a first-order multi-objective optimization approach is adopted. The gradients of the expected loss function, required for the optimization, are analytically derived using the very efficient Adjoint Variable method. This considerably improves the computational efficiency of the methodology. The efficacy of the framework is illustrated with a 2D four storey frame and an eight-storey 3D asymmetric building.

1. Introduction

Recent seismic events have shown that, when it comes to modern countries with modern seismic codes, loss of human lives due to collapse of buildings is considerably smaller compared to that in the past. For example, the 1994 Northridge and the 2011 Christchurch earthquakes caused a total of 57 and 185 deaths, respectively. As saving human lives has been the major task of earthquake engineering, this is indeed an achievement for the structural engineering community. However, with the relatively small number of deaths due to these events, came huge monetary losses. The 1994 Northridge and 2011 Christchurch led to losses estimated at ~ US \$44 billion and ≥ ~NZ \$40 billion (corresponds to approximately 20% of the GDP), respectively (direct and indirect). This motivates a design considering expected losses in parallel to reducing loss of human lives [2].

Adopting such a design approach is necessary for new buildings, where new technologies to limit damage could be easily included. One such loss based design approach is the *Loss Optimization Seismic Design*, commonly referred as LOSD [3,4]. This may highly affect the losses to be expected in the far future. Nonetheless, in the foreseen future, most buildings to experience earthquakes are ones that have already been designed and built based on the sole goal of saving human lives. Thus, new technologies and design approaches for their retrofitting are required to reduce expected losses.

Such new technologies for seismic protection have shown to be

beneficial for mitigation of damage to regular structures [5–9]. These technologies may even be more beneficial for mitigation of damage to irregular structures [10–15]. It has been observed that such irregular structures are more seismically vulnerable than their regular counterparts [16]. For example, many of the buildings to be damaged due to the 2010 Chile earthquake presented some source of irregularity (either vertical, horizontal or both) [17]. This is not surprising as plasticity and damage are well known to concentrate in the vicinity of irregularity, while presenting very high local ductility demands [18]. This is one of the reasons that new technologies for seismic damage mitigation, if applied wisely, could very well reduce such damage in irregular structures.

Fluid viscous dampers (FVDs) are such a new technology. They have been shown to be very efficient in reducing inter-story drifts in frame structures [6]. Inter-story drifts are the main engineering demand parameter (EDP) associated with structural damage and damage to drift sensitive non-structural components. Thus, FVDs are expected to efficiently reduce seismic losses. In addition to reducing inter-story drifts, a careful use of linear FVDs for seismic retrofitting has been shown to efficiently reduce total accelerations (e.g. Ref. [19]). Such accelerations are the main EDP associated with damage to acceleration sensitive non-structural components. This further enhances the efficiency of FVDs in reducing seismic losses. As a careful use of FVDs for seismic retrofitting may reduce total accelerations and forces, or at least may not increase them as other technologies, it may prevent the need for columns and

[☆] This paper is an extension of the conference paper by Puthanpurayil et al. [1].

* Corresponding author.

E-mail address: lavan@technion.ac.il (O. Lavan).

<https://doi.org/10.1016/j.soildyn.2019.105765>

Received 19 December 2018; Received in revised form 14 July 2019; Accepted 15 July 2019

0267-7261/ © 2019 Elsevier Ltd. All rights reserved.

foundation strengthening [6,20]. This may have a huge effect on the initial cost of retrofitting. It should be noted that the performance of the structure may be very much affected by the damping distribution [21]. Thus, there is much room for damping optimization. This is expected to be even more pronounced in irregular structures.

Indeed, many approaches for the optimal design of FVDs, especially for the purpose of seismic retrofitting of frame structures, have been proposed over the years. Early works targeted the design of the dampers based on energy considerations (e.g. Zhang and Soong [22–33]). For example, the SSA [33] and the SSSA [25] algorithms focused on maximizing the energy dissipated by the dampers. Using these approaches the designer sequentially adds dampers at the locations where they are expected to dissipate the most energy. Another suit of approaches aimed at minimizing some energy (elastic, kinetic) responses of the parent structure [22,23]. Designing based on energy measures makes a lot of sense. It is believed, also by the authors, that such a design may reduce some overall response measures of the structure. Nonetheless, the actual responses of interest remain un-known. Furthermore, while overall responses may reflect on the performance of regular buildings, this is not the case when it comes to irregular buildings. As noted above, the behaviour of irregular structures is characterized by excessive local deformation demands at the region of irregularity. Thus, while some distributions of dampers may reduce some overall performance measure, the local deformations at the region of irregularity may not be efficiently mitigated. This may, in some cases, lead to collapse, or a financial total loss of the structure where the structure cannot be fixed after an event due to excessive local deformations.

A step forward was made when design methodologies based on actual EDPs were proposed (e.g. Refs. [14,19,22,30,32,34–51]). For example, Takewaki [38] proposed using the sum of amplitudes of inter-story drifts' transfer function evaluated at the natural period of the structure. Lavan and Levy [45] suggested using the envelope peak inter-story drifts at selected locations as performance measures (each one separately or the maximum between all). This was an important step forward as, with some of these approaches, the design could be made for a desired seismic performance of the building, from an engineering point of view. That is, local deformation demands could be treated explicitly, and collapse or financial total loss could be prevented.

Inter-story drifts are very important EDPs that structural engineers understand very well. They serve as a good measure for how close the building is to collapse (physical or financial). Furthermore, they reflect on the damage state of the structural system as well as some non-structural components. However, stakeholders and decision makers are often not engineers. Thus, they may not have a sense to the implications of inter-story drifts, or any other EDP. In addition, EDPs are indeed correlated to damage and, in turn, to losses. Nonetheless, they do not directly represent losses, that are the ones one wishes to reduce (assuming collapse and loss of human lives are prevented). This makes the design based on EDPs somewhat limited as engineers, that understand EDPs, are not the ones to make the decisions. On the other hand, the decision makers do not understand EDPs. Thus, to allow the decision makers make their decisions based on parameters they understand, the design should be based on expected losses.

A design based on financial considerations has been proposed by Park et al. [48]. They made use of a genetic algorithm (GA) approach for the minimization of the life-cycle cost of structures equipped with visco-elastic dampers. The life-cycle cost combines the upfront cost (initial cost of the structure with the dampers) with the expected losses (or damage cost). The expected damage cost required for the life-cycle cost evaluation was evaluated using a frequency domain analysis of the structure. That is, a linear model of the structure and the dampers is adopted. Such a model can be justified in many cases, when dampers are added to the structure. A year later, Dargush and Sant [43] developed a GA based computational framework for the optimal design of dampers in nonlinear shear frames. They considered VDs, VEs and yielding devices. Their fitness function comprised of the economic

benefit derived from the structure, the negative of cost of the dampers and the negative of a damage cost associated with the behaviour of the structure under the considered seismic environment. The framework was able to trace trends in the characteristics of optimal designs. The algorithm tended to favour the rate dependent devices over the yielding devices. Recently, GA frameworks for the optimization of designs based on financial considerations have been proposed as well [52,53]. They minimized the life-cycle cost of retrofitted nonlinear buildings. A closely related measure for the expected losses is the probability of exceeding a given damage state. In this direction Altieri et al. [54] minimized a measure of the retrofitting cost using fluid viscous dampers while constraining the probability of failure of the retrofitted structure. For the optimization, they made use of a constrained optimization by linear approximation method.

While the approaches mentioned above for financial based optimization present an important step forward, the optimization of the problem using zero order methods often requires a large number of function evaluations. In the cases considered, each function evaluation (computation of the life-cycle cost or probability of failure) requires multiple structural analyses (in some approaches nonlinear time-history analyses). Thus, there is a need for a more computationally efficient optimization approach. Furthermore, it would be beneficial for the decision maker to separate the initial cost of retrofitting from the expected losses. Indeed, this can be done by minimizing the initial cost and constraining the expected losses or vice versa. Nonetheless, this will enforce deciding *a priori* on an upper bound for either the initial cost or the expected loss. Such a decision, that is made *a priori*, may have a huge effect on the resulted optimal design. Thus, an alternative approach should be taken.

A very well-established way of enabling the decision to be made without setting any parameter *a priori* is by the notion of Pareto optimality [55]. The philosophy behind Pareto optimality is that rather than attempting to identify a single optimal design, one seeks to determine an entire family of designs. For each of these designs an improvement in one objective can be achieved only with a degrade in at least one other objective. This philosophy has been adopted in the context of seismic retrofitting while minimizing both inter-story drifts and total accelerations by Lavan and Dargush [19]. They indicated that using a multi-objective optimization approach may sometimes have a huge benefit over single objective optimization. This is because the selection of the solution can be done with the whole picture at hand, without setting any parameters *a-priori*. This is because some optimization problems may be very sensitive to the choice of values set for some parameters.

An efficient approach for the multi-objective optimal design of seismic retrofitting using FVDs is the purpose of this paper. It is suggested to adopt the initial cost as one objective and the expected losses as the other, within a multi-objective framework. Within this framework, the Pareto front is efficiently computed using a gradient based approach. Thus, the Pareto front can be practically obtained within a reasonable time using a personal computer. With the Pareto front, the decision maker can choose the best compromise between two competing objectives he understands, while having the whole picture at hand. This may give the decision maker the freedom of choosing the best compromise between the initial investment and the expected losses, without setting any parameter *a priori*.

2. Problem formulation

In this paper a multi-objective loss optimization framework is proposed. The problem deals with the seismic retrofitting of existing frame structures using fluid viscous dampers. Fluid viscous dampers are potentially allocated in various locations determined by the engineer considering architectural and functional constraints. Their damping coefficients serve as the design variables. Although the number of potential locations for the dampers may be large, a particular case is when

the optimization sets a zero value for the damping coefficient of a given potential damper. This indicates that no damper is required at the specific location. It should be noted that in the current paper the damping coefficients are continuous variables. Hence, some post-processing may be required from the engineer to group dampers of close sizes to a single size group. An alternative approach to that for the case of single objective optimization is given in Refs. [56–59].

The problem discussed is a bi-objective problem. The two competing objectives are the initial cost of retrofitting and the today's worth of the expected losses. A Pareto front with these two objectives allows the decision maker to choose the best compromise between the expenses he needs to meet today versus today's worth of the financial losses he is expected to suffer in the future. From physical reasons, non-negativity constraints are added on the damping coefficients of the dampers.

2.1. Design variables and the behaviour of fluid viscous dampers

In this paper, the general force-velocity relation of fluid viscous dampers to be designed is given by:

$$F = C \operatorname{sgn}(\dot{x}) |\dot{x}|^\alpha \quad (1)$$

where,

F represents the damper force, C represents the damper coefficient, \dot{x} represents the velocity and α represents the velocity exponent ranging from 0.15 to 2.0. It is well accepted that with a small exponent, α , the force in a damper does not increase considerably with an increase of the velocity between its ends. Thus, if a stronger earthquake than designed for takes place, the forces the dampers apply to their neighbouring structural elements are limited. As a result, brittle failure may be avoided. This is in contrast to linear dampers (i.e. with an exponent of one) where the force in the damper increases linearly with its relative end velocity. Nonetheless, it has been also shown that, with a small exponent, a stronger earthquake than designed for would lead to much larger deformations in the building compared to the same building retrofitted with linear dampers [60,61]. Thus, in the context of this paper, linear dampers are to be optimized. With the value of α set to one, the sole parameter that controls the behaviour of the damper is its damping coefficient. The damping coefficients of the various dampers (potentially allocated in various locations in the building) are set as the design variables. It should be noted that damper limit states may also affect the behaviour of the retrofitted structure (see e.g. Ref. [62]. Nonetheless, in this work the damper is an element to be designed, and not an element with given properties. Thus, the designer could assess the force and stroke demands from the damper and design it accordingly.

2.2. Retrofitting cost estimation

Various levels of detail have been proposed for the retrofitting cost of frames using fluid viscous dampers. In the present work, the sum of added damping coefficients is adopted. Under some circumstances, this may be a reasonable approximation for the cost of manufacturing the dampers (see e.g. Ref. [57]). It should be noted that retrofitting cost estimations that account for the prototype testing of a damper from each group of similar dampers, as well as for the cost of installation of each damper, are available (see e.g. Ref. [57]). Nonetheless, these require tools and techniques from topology optimization that are not yet suited for a gradient based multi-objective optimization.

Formally, the retrofitting cost estimation adopted in this paper can be written as follows:

$$\Gamma(c_d) = \sum_{i=1}^{N_{dampers}} c_{d,i} \quad (2)$$

where $\Gamma(c_d)$ is the total damper quantity which represents the total cost

of dampers, $c_{d,i}$ is the damper coefficient and $N_{dampers}$ represent the total number of dampers.

2.3. Expected loss computation

This section summarizes detail loss assessment framework as reported in Aslani and Miranda [63]. In classical detail loss assessment framework (PEER format), the expected annual loss or the loss expected over a period of time is computed as,

$$E[L_T] = \frac{1 - e^{-\lambda t}}{\lambda} \int_0^\infty E[L_T|IM] dv(IM) \quad (3)$$

where,

$E[L_T]$ is the expected annual loss; λ is the discount rate; t is the period for which the rate is applied; it can be the design life of the building or remaining life of the structure; $E[L_T|IM]$ is the expected loss conditioned on the intensity measure IM ; $v(IM)$ is the mean annual rate of exceedance of the intensity measure.

$E[L_T|IM]$ can be divided into two components,

$$E[L_T|IM] = E[L_T|NC, IM]P(NC|IM) + \text{Total building value} \times P(C|IM) \quad (4)$$

Over here,

$E[L_T|NC, IM]$ is the expected loss in non-collapse case; $P(NC|IM)$ is the probability of non-collapse for the specific ground motion intensity; $P(C|IM)$ is the probability of collapse for the specific ground motion intensity.

The addition of viscous dampers reduces the collapse probability considerably in a major event. So, it could be argued that only non-collapse case need be considered while using viscous dampers which means no probability of collapse be computed. An alternative approach is to use a modified framework in which the whole loss is computed in such a way that there is no collapse and the effect of collapse is introduced through a Heaviside step function in such a way that when drift exceeds a certain value in any of the ground motions considered, it is deemed as a total loss. This approach is adopted in the present study. So first the loss is computed assuming no collapse and then the obtained equation is modified by introducing the Heaviside step function term. This aspect is described in more detail in section 2.3.1.

Assuming no global collapse ($P(NC|IM) = 1.0$), eq. (4) becomes,

$$E[L_T|IM] = E[L_T|NC, IM] \quad (5)$$

Now

$$E[L_T|NC, IM] = \sum_{j=1}^N a_j (E[L_j|IM]) \quad (6)$$

Over here,

a_j is the cost of a new j^{th} component; $E[L_j|IM]$ is the expected loss of the j^{th} component conditioned on the ground motion intensity. Note that from here on "NC" is not being explicitly stated as the computation is only done for the non-collapse case.

Now the expected loss of the j^{th} component conditioned on the ground motion intensity is given as,

$$E[L_j|IM] = \int_0^\infty E[L_j|EDP_j] dP(EDP_j \geq edp|IM) \quad (7)$$

Over here,

$E[L_j|EDP_j]$ is the expected loss in the j^{th} component when it is subjected to an EDP_j when no collapse occurs; $P(EDP_j \geq edp|IM)$ is the probability of the EDP exceeding edp in the j^{th} components when no collapse occurs. Again,

$$E[L_j|EDP_j] = \sum_{i=1}^m E[L_j|DS_i] P(DS = ds_i|EDP_j) \quad (8)$$

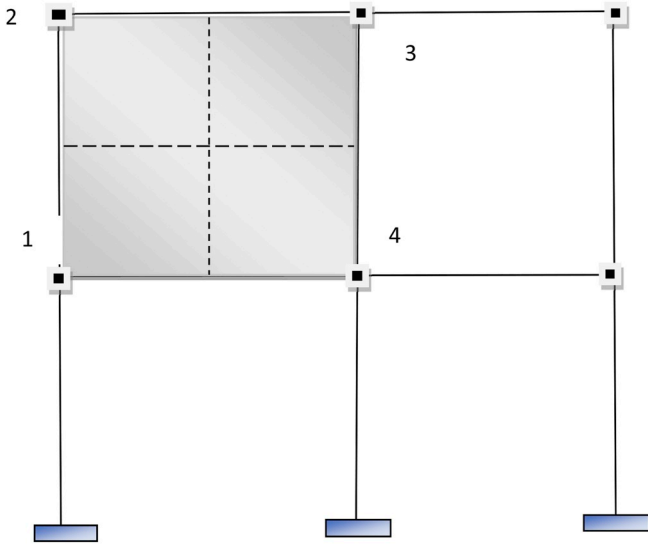


Fig. 1. two storey two bay frame with partition wall.

$E[L_j|DS_i]$ is the expected loss conditioned on damage state i . In other words, it is the loss in the j^{th} component when the component is in damage state i and can be obtained from experimental database [63]. $P(DS = ds_i|EDP_j)$ is the probability of the j^{th} component being in damage state ds_i when the EDP_j is experienced by the j^{th} component and is given as follows [63].

$$\left. \begin{aligned} P(DS = ds_i|EDP_j) &= P(DS \geq ds_i|EDP = edp) - P \\ &\quad (DS \geq ds_{i+1}|EDP = edp) \\ P(DS \geq ds_i|EDP = edp) &= \Phi \left[\frac{Ln(edp) - Ln(EDP_{mean})}{\sigma_{LnEDP}} \right] \end{aligned} \right\} \quad (9)$$

Here, σ_{LnEDP} is the logarithmic standard deviation of EDP.

A simplified loss computation methodology is adopted for the present study. A discrete *lumped loss estimation approach* in which loss incurred is computed as a function of the structural response of each degree of freedom is used for the present study. This is mainly motivated from the studies of Ramirez and Miranda [64] in which a storey-based loss estimation was introduced as a more pragmatic framework for performing loss estimation. To further illustrate this aspect, Fig. 1 represents a two bay two storey frame with a partition wall in the first floor level.

It is very clear that damage to the partition wall will be a function of the inter-storey drift of these nodes. Lumping of loss philosophy assumes that if the value of the partition wall is say χ then each node connecting it will be assigned an equal share of the value; i.e. $\chi/4$. In other words, an influence factor is introduced which transforms the value of each component and lumps it to a specific degree of freedom. The loss incurred will then be a function of the inter-storey drift associated with that degree of freedom. This type of approach may be conveniently adopted for predominantly drift sensitive non-structural components mainly because all the drift sensitive items would be directly or indirectly connected to the parent structural members.

Damage to acceleration sensitive items would be a function of the specific floor mass acceleration alone; so, losses may be lumped to the specific floor masses and will be very similar to the Ramirez and Miranda [64] approach. Losses may also be lumped to the acceleration felt by a specific degree of freedom by computing/assessing the proximity of the structural node to the component under consideration.

2.3.1. Simplified loss framework including collapse consideration

The first simplification comes from the fact that only intensity-based loss assessments are used in this study. So only EDP corresponding to a specific intensity of ground motion is adopted and the resulting loss is

termed as total expected loss. Except for step 8, all the steps which are detailed below are adopted from Aslani and Miranda [63] and Ramirez and Miranda [64]. The steps are as follows:

1. Perform linear/nonlinear time history analyses using n ground motions compatible with a target spectrum.
2. Compute the mean response history from the n response histories
3. For the j^{th} component, determine the probability of being in a damage state by computing eq. (9).
4. Determine $E[L_j|NC, DS_i]$, expected loss of j^{th} component conditioned on damage state i from the loss database. For the present study the loss database given in Aslani and Miranda [63] is adopted.
5. For the j^{th} component, compute $E[L_j|EDP_j]$, expected loss of j^{th} component subjected to EDP_j for no collapse state using eq. (8).
6. Repeat steps 3–5 for all components
7. Compute the total normalized expected loss conditioned on EDP for no collapse as follows,

$$\left. \begin{aligned} E[L_T|EDP] &= \sum_{j=1}^N \beta_j E[L_j|EDP_j] \\ \beta_j &= T \alpha_j \end{aligned} \right\} \quad (10)$$

where T represents the spatial influence factor which determines the lumping.

8. Introduce the Heaviside function to reflect the collapse scenario as shown below,

$$\left. \begin{aligned} \Psi &= E[L_T|NC, EDP] H(d_{al} - X) + Total\ building\ value \times H(X - d_{al}) \\ X &= Env \left(\max_i \left(\left\{ \max_t (abs(\mathbf{H}_T \mathbf{u}_1(t))), \max_t (abs(\mathbf{H}_T \mathbf{u}_2(t))), \dots, \max_t \right. \right. \right. \\ &\quad \left. \left. \left. (abs(\mathbf{H}_T \mathbf{u}_{N_{gm}}(t))) \right\} \right) \right) \end{aligned} \right\} \quad (11)$$

Over here, Ψ represents the expected total loss conditioned on EDP, d_{al} refers to the capping drift, H refers to the Heaviside step function, $\mathbf{H}_T \mathbf{u}_i(t)$ refers to the drift, Env refers to envelope. In eq. (11) X represents the envelope of the maximum of the maximum at any instant in any storeys. The use of Heaviside step function reflects the fact that when the computed drift exceeds an allowable capping drift, total loss is assumed. It should be understood here that, exceeding this capping drift does not mean physical collapse of the structure, but mainly relates to a situation of complete financial loss as the structure gets written off due to non-reparability or non-usability. So, the selection of capping drift is very important. Even the definition of non-reparability or non-usability is subjective and depends on lots of other associated societal aspects.

First order gradient-based optimization schemes are used for the optimization framework described in the next section. Because of this, to integrate seismic loss into this framework, the expected loss functions need to be described as smooth functions. One way to describe the functions is by using interpolation techniques. The simplest interpolations that can represent these functions are polynomial functions. Using polynomial functions, expected loss function of the j^{th} component is expressed as,

$$E[L_j|NC, EDP_j] = \sum_{i=1}^k A_i (EDP_j)^{\eta_i} \quad (12)$$

Here, A_i, η_i are the constants in the polynomial. These constants differ for different components and need to be explicitly evaluated.

A more robust methodology of interpolation would be to use cubic spline functions; but to the knowledge of the authors, as this the first time an attempt is initiated to integrate the seismic loss aspect into the first order gradient multi-objective optimization framework, the

simplest polynomial based interpolation technique is adopted in this study; considering the other uncertainties associated with the loss estimation process, this methodology is deemed to be acceptable.

2.4. Optimization problem formulation

This section presents the generic framework for multi-objective optimization. First order gradient-based schemes are employed to solve the optimization problem. The optimization problem involves minimizing simultaneously the initial cost described in section 2.2 and the expected total loss described in 2.3. In this study, seismic losses due to downtime and injury are not accounted for; thereby resulting in underestimation of the benefits of optimal intervention.

The framework presented here is applicable equally to strengthening existing buildings and to new buildings. In a new building, both stiffness and damping may be considered as variables and maybe optimized to achieve a target performance; but in this present work only the added damping is considered as the variable. If only damping is considered as the variable, then the initial cost in the case of enhancing seismic performance with viscous dampers can be assumed as the cost of added dampers and their installation.

The optimization problem is formulated as given below,

$$\begin{aligned}
 & \min(\Gamma(\mathbf{c}_d), \Psi(\mathbf{c}_d)) \\
 & \text{here,} \\
 & \Psi = \{H(X - d_{al})\} \times C_{total} \\
 & + \{H(d_{al} - X)\} \times \sum_{j=1}^{N_d} c_j \sum_{i=1}^k A_i \left(\frac{1}{N_{gm}} \sum_{r=1}^{N_{gm}} \left\{ \max_t(\text{abs}(\mathbf{H}_T \mathbf{u}_r(t))) \right\} \right)^{\eta_i} \\
 & \text{where } \mathbf{u}_r(t) \text{ follows} \\
 & \mathbf{M}\ddot{\mathbf{u}}_r(t) + [\mathbf{C} + \mathbf{C}_{damper}(\mathbf{c}_d)]\dot{\mathbf{u}}_r(t) + \mathbf{K}\mathbf{u}_r(t) = -\mathbf{M}\mathbf{r}\ddot{u}_{g,r}(t) \\
 & \mathbf{u}_r(0) = 0; \dot{\mathbf{u}}_r(0) = 0 \\
 & 0 \leq \mathbf{c}_d \\
 & r = 1 \rightarrow N_{gm} \\
 & X = \text{Env} \left(\max_i \left(\left\{ \max_t(\text{abs}(\mathbf{H}_T \mathbf{u}_1(t))), \max_t(\text{abs}(\mathbf{H}_T \mathbf{u}_2(t))), \dots, \max_t(\text{abs}(\mathbf{H}_T \mathbf{u}_{N_{gm}}(t))) \right\} \right) \right) \\
 & \forall \ddot{u}_{g,r}(t)
 \end{aligned} \tag{13}$$

In eq. (13) H refers to the Heaviside step function; \mathbf{H}_T refers to the drift transformation matrix; \mathbf{c}_d refers to the damper vector; \mathbf{u}_r , $\dot{\mathbf{u}}_r$ and $\ddot{\mathbf{u}}_r$ are displacement vector, velocity vector and acceleration vector for the r^{th} ground motion; N_{gm} represents the number of ground motions; \mathbf{M} , \mathbf{C} and \mathbf{K} are the mass, inherent damping and stiffness matrices; $\mathbf{C}_{damper}(\mathbf{c}_d)$ is the added viscous damper matrix; \mathbf{r} is the directionality vector; $\ddot{u}_{g,r}$ is the r^{th} ground motion acceleration vector; C_{total} is the total cost of the structure; c_j is the cost of the j^{th} component; A_i is the constant multiplier associated with the loss function, η_i represents the power, N represents the degrees of freedom. Eq. (13) represents the simultaneous minimization of damper quantities and expected total loss. The effect of collapse is considered by incorporating the Heaviside step function with a kernel function comprising of capping drift d_{al} and envelope drift.

Heaviside step function is used in eq. (13) to introduce a control on the limiting acceptable loss. The kernel of the Heaviside step function involves the envelope computed drift which is basically the maximum of the drifts at all levels considering all ground motions and the allowable acceptable capping drift d_{al} . In the present study, d_{al} is chosen to make the frame remain predominantly linear.

One aspect of eq. (13) is that when the envelope computed drift exceeds the d_{al} , it is assumed that the structure would be completely written off. To emphasize this point, in the recent 2016 Kaikoura earthquake in New Zealand, one multi-story building was demolished

mainly classing it as non-repairable. The main damage in the building was in one of the columns where there was a reasonable hinge formation. Albeit the experienced engineer's belief that it could be repaired, and building be re-used, the building was marked for demolition mainly because the health and safety laws prevented the workers from going inside the building to do the repair. This is a very significant societal aspect which drives what is deemed as acceptable in the modern society. The selection of d_{al} in eq. (13) may be used to indirectly reflect these societal aspects. This epitomizes the significance of eq. (13) from a pragmatic view point as it gives direct control of allowable acceptable damage to the designer.

Similar justifications for this approach may again be obtained from the Christchurch sequence of earthquakes. It had been observed during the Christchurch sequence of earthquakes that so many buildings though did not collapse had to be demolished as the damage was classed as non-repairable; it was also observed that owners or stake holders had a strong tendency to write off their assets (buildings) when it suffered moderate repairable inelasticity mainly because they could claim insurance (Personal communications with experienced engineers). There are also so many other non-technical reasoning that maybe attributed to the demolition of many buildings. This is a huge economic burden on the society and gives a strong motivation for forcing the capping drift to a value so that the system is predominantly elastic in a design event.

Eq. (13) presents a nonlinear optimization problem. In the present study, this problem is solved by discretizing the nonlinear objective functions and are solved by using an aggregate gradient based methodology [65].

3. Optimization procedure

The problem presented in Eq. (13) is a multi-objective optimization problem. Most of the optimization approaches for solving such a problem are zero-order methods. That is, they require the ability to evaluate the values of the objective functions only (and constraints, if applicable) for given designs. Such approaches usually require the evaluation of the objective functions for many designs. For the problem at hand, where the evaluation of one of the objective functions requires multiple time-history analyses, this leads to a tremendous computational effort. Recently, Izui et al. [65] presented a first-order multi-objective optimization approach. As a first-order optimization method, it requires the evaluation of not only the objective functions for given designs, but also their gradients w.r.t the design variables. This may be mistakenly thought of as a disadvantage of the approach. However, it has been observed that this approach requires the evaluation of the objective functions and their gradients for a much smaller number of designs compared to zero-order methods (see e.g. Izui et al., [65,66]). Thus, if the gradients could be efficiently evaluated, this approach is very beneficial, from a computational effort point of view. In addition, the Pareto fronts that this approach converges to have been shown to dominate those obtained using GA, as well as more diverse.

In the next sections, the application of the approach proposed by Izui et al. [65] for the problem at hand, as well as the gradient derivation, will be presented in detail.

3.1. Main stages of the aggregate gradient-based methodology (adapted from Izui et al. [65])

In much similarity to GA, the gradient based approach starts with a set of initial designs and generates a new set of designs (or a new generation) in each iteration of the optimization. In each iteration, the objective functions and their gradients are evaluated for each design. In turn, design is updated using the information from all other designs. This is done by converting the multi-objective problem for each design into a single objective problem using an adaptive weighting technique. The weights are computed while considering the locations of all the

designs within the iteration in the design space. The obtained single objective problem for each design is then solved using a sequential linear programming (SLP) method and the design variables are updated. Brief overview of the main stages of the method as applied to the viscous damper optimization is as follows:

Step 1. Selection of a suite of ground motions matching the specified intensity

An ensemble of ground motions is selected to match the target mean spectrum corresponding to the specific intensity level of interest. It must be noted that the procedure outlined in this section is equally applicable to time-based assessments in which case the expected annual loss will be minimized instead of the total expected loss used in the present study.

Step 2. Initialization of design variables and generation of initial design points

Design point is basically obtained by computing the two objective functions given in eq. (13) assuming a specific random distribution for the design variable which are the damper coefficients. Mathematically this means, for q design variables (damper coefficients), generate K design points using random values for the design variables. For e.g. if we assume $q = 2$ and $K = 7$, then there are seven random distributions of the two dampers and each design point in the objective function space as shown in Fig. 2 corresponds to evaluation of the objective functions in eq. (13) subject to the constraint on the damper coefficients.

Step 3. Compute weighting coefficients as per Data Envelopment Analysis (DEA)

To generate the Pareto front, the design points shown in Fig. 2 need to move towards the Pareto frontier that is closest to its current position in the objective function space. But as the Pareto frontier is not known prior to optimization calculation, the points in the objective function space need to be updated using an adaptive weighting method. Only a very brief detail is given in this step and for details interested readers should refer to Izui et al. [65].

DEA computes the efficiency of the M^{th} point by solving a linear programming problem as,

$$\begin{aligned} \min(\lambda^M) &= \sum_{i=1}^m w_i^M f_i^M \\ \text{Subject to,} & \left\{ \begin{array}{l} \sum_{i=1}^m w_i^M f_i^k \geq 1 \\ w_i^M \geq 0 \end{array} \right. \quad \left\{ \begin{array}{l} \text{for } k=1,2,\dots,K \end{array} \right. \end{aligned} \quad (14)$$

Here f_i^k is the k th point's i th objective function value and w_i^M represents the weighting coefficients.

Step 4. Compute the sensitivities of the objective functions for the M^{th} point

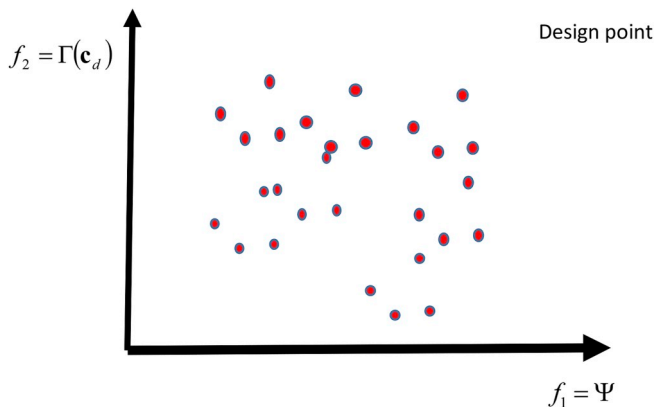


Fig. 2. Objective function space.

Gradient for the objective function Γ^M is trivial as it is a direct function of the damping vector c_d and the sensitivity will return a vector **1**. But the gradient of the objective function Ψ^M is not trivial. One way to determine the gradient is by finite difference approach; but this has serious limitations in terms of computational demand as it requires $n + 1$ analysis for n design variables. So, in the present study, gradients are computed analytically using the Adjoint Variable method as outlined in section 3.1.2.

Step 5. Update the design variables of the M^{th} point

For each point M , a minimization of the weighted sum of the objective functions is done using sequential linear programming (SLP) and the design variables are updated. SLP uses a suitable move limit to arrive at the updated value of the design variable. For the M^{th} point we get,

$$\min f^M = \sum_{i=1}^m w_i^M \sum_{j=1}^n \frac{\partial f_j(c_d^M)}{\partial c_{dj}} c_{dj} \quad (15)$$

Subject to

$$c_d^L \leq c_d \leq c_d^U \quad (16)$$

Here f^M is the weighted sum of the objective functions, c_d^M is the design variable vector of the M^{th} point before updating, c_d^L and c_d^U are the lower and upper move limits of the design variable. If $M = n$ then proceed to step 6, else adopt $M = M + 1$ and proceed to step 4. For more details on this step interested readers should refer Izui et al. [65].

Step 6. Check for termination condition.

If termination condition is satisfied (maximum number of iteration), the procedure ends else returns to step 2.

3.1.1. Gradient derivation

In this section an efficient way to compute $\nabla_{c_d} \Psi$ is described in detail.

The gradient derivation in this paper incorporates the differentiated-discretize version of the Adjoint Variable Method (AVM) approach as outlined in the Lavan and Levy [45] and Jensen et al. [74]. To derive the analytical gradients by AVM approach, non-differentiable functions like \max and abs in eq. (13) need to be replaced by differentiable functions. In this study a p type norm is used.

Using the differentiable p type norm version, $\mathbf{d}_{est,r} = \max(\text{abs}(\mathbf{H}_T \mathbf{u}_r(t)))$ is replaced as,

$$\mathbf{d}_{est,r}(t_f) = \left(\frac{1}{t_f} \int_0^{t_f} D^p(\mathbf{H}_T \mathbf{u}_r(t)) dt \right)^{\frac{1}{p}} \mathbf{1} = D^{\frac{1}{p}}(\mathbf{d}_{mp,r}(t_f)) \mathbf{1} \quad (17)$$

$r \rightarrow 1 \text{ to } N_{gm}$

where

$$\mathbf{d}_{mp,r}(t_f) = \frac{1}{t_f} \int_0^{t_f} D^p(\mathbf{H}_T \mathbf{u}_r(t)) dt \mathbf{1} \quad (18)$$

p is a large positive even number; t_f is the final time.

Now in differential format eq. (18) can be written as,

$$\left\{ \begin{array}{l} \dot{\mathbf{d}}_{mp,r}(t_f) = \frac{1}{t_f} D(\mathbf{H}_T \mathbf{u}_r(t))^p \cdot \mathbf{1} \\ \mathbf{d}_{mp,r}(0) = \mathbf{0}; \end{array} \right. \quad (19)$$

Now to compute the $\text{Env} \left(\max_i(\dots) \right)$, a weighted approach is adopted [45].

$$Env \left(\max \left(\max_t (abs(H_T \mathbf{u}_1(t))) \right), \dots, \max \left(\max_t (abs(H_T \mathbf{u}_{N_{gm}}(t))) \right) \right) \\ = \frac{\sum_{r=1}^{N_{gm}} \mathbf{1}^T \cdot \left\{ D(\mathbf{d}_{mp,r}(t_f))^{\frac{1}{p}} \right\}^{q+1} \cdot \mathbf{1}}{\sum_{r=1}^{N_{gm}} \mathbf{1}^T \cdot \left\{ D(\mathbf{d}_{mp,r}(t_f))^{\frac{1}{p}} \right\}^q \cdot \mathbf{1}} \quad (20)$$

where q is a large positive value.

Introducing eqs. (19) and (20) in eq. (13), and taking the variation of the augmented objective function results in a set of differential equations and boundary conditions when all multipliers of variations except δ_{c_d} are equated to zero. This is given as follows,

$$\left. \begin{aligned} \mathbf{M}\ddot{\lambda}_r(t) - \mathbf{C}\dot{\lambda}_r(t) + \mathbf{K}\lambda_r(t) &= -\frac{\partial \phi_r}{\partial \mathbf{u}_r} \chi_r(t_f) = \frac{\partial \phi_r}{\partial \mathbf{u}_r} \{\mathbf{Q}_{1,r} + \mathbf{Q}_{2,r} + \mathbf{Q}_{3,r}\} \\ \mathbf{C}\lambda_r(t_f) - \mathbf{M}\dot{\lambda}_r(t_f) &= 0 \\ \mathbf{M}\lambda_r(t_f) &= 0 \\ \lambda_r(t_f) = \dot{\lambda}_r(t_f) &= 0 \\ \phi_r &= \dot{\mathbf{d}}_{mp,r}(t_f) - \frac{1}{t_f} D^p (\mathbf{H}_T \mathbf{u}_r(t)) \mathbf{1} \\ \frac{\partial \phi_r}{\partial \mathbf{u}_r} &= -\frac{p}{t_f} \cdot \mathbf{H}_T^T \cdot D^{p-1} (\mathbf{H}_T \mathbf{u}_r(t)) \end{aligned} \right\} \quad (21)$$

where λ_r and χ_r are the Lagrangian multipliers.

Solving eq. (21),

$$\frac{\partial \hat{\Psi}}{\partial \mathbf{c}_d} = \sum_{i=1}^{N_{gm}} \int_0^{t_f} \lambda_i^T(t) \frac{\partial \mathbf{C}}{\partial \mathbf{c}_d} \dot{\mathbf{u}}_i(t) dt \quad (22)$$

Eq. (22) represents the analytical gradients which is used in step 4 of the main optimization framework.

4. Numerical study

4.1. Four storey frame

The first example makes use of a 2D four-storey reinforced concrete setback frame. This frame is based on a four storey two bay frame that was designed in accordance with Eurocode 8 (EC8) and Eurocode 2 (EC2) (see Ref. [67]). However, in this example, the left bay of the fourth storey was removed. The frame is designed for high seismicity assuming

Table 1.0
Geometric properties.

Member number	Width of the member (mm)	Depth of the member (mm)
1,6,11,2,7,12,15,3,8,13, 16	450	450
4,5,9,10,14,17	300	450

Table 2.0
Nodal Mass [67].

Floor level	Mass per node (kg)
1st floor	29,800
2nd -3rd floor	29,500
4th floor	19,600

a PGA of 0.3 g. The geometric dimensions of the frame with the location of the partition walls and the arrangement of the dampers are given in Fig. 3. It should be noted that in the analysis, partition wall was not modelled and only the bare frame with the dampers are analyzed.

Dynamic Young's modulus of concrete is assumed as $3.5 \times 10^{10} \text{Nm}^{-2}$. Geometric properties and nodal masses are given in Tables 1 and 2.

The proposed framework is very generic and can include any number of components; but as the whole purpose of this example is to demonstrate the multi-objective optimization framework, only loss to partition walls and beam column joints are included in the study. Expected total loss is computed as described in section 2.3.1.

Realistic normalized cost for the two types of components considered in the loss is adopted from the Rawlinson's cost estimation schedule [72]. The frame is assumed to be part of a three-dimensional building system with floor area of 100m^2 per floor up to 3rd floor and 50m^2 in the fourth floor. As per the Rowlinson's pricing manual 2012 (Rowlinson database, New Zealand), assuming the architectural functionality as hospitality, the floor cost is assumed to be $\$4750/\text{m}^2$ which would then total to $\$475,000$ per floor up to third floor and $\$237,500$ for the fourth floor. The total estimated cost would be $\$1,662,500$. For this present example, it is assumed that 70% of this total estimated cost is assigned to the frame under consideration which would amount to $\$1,163,750$. It should be remembered that this total cost estimate given by Rawlinson's schedule consists of approximate cost of all the components and as only two components (beam column joints and

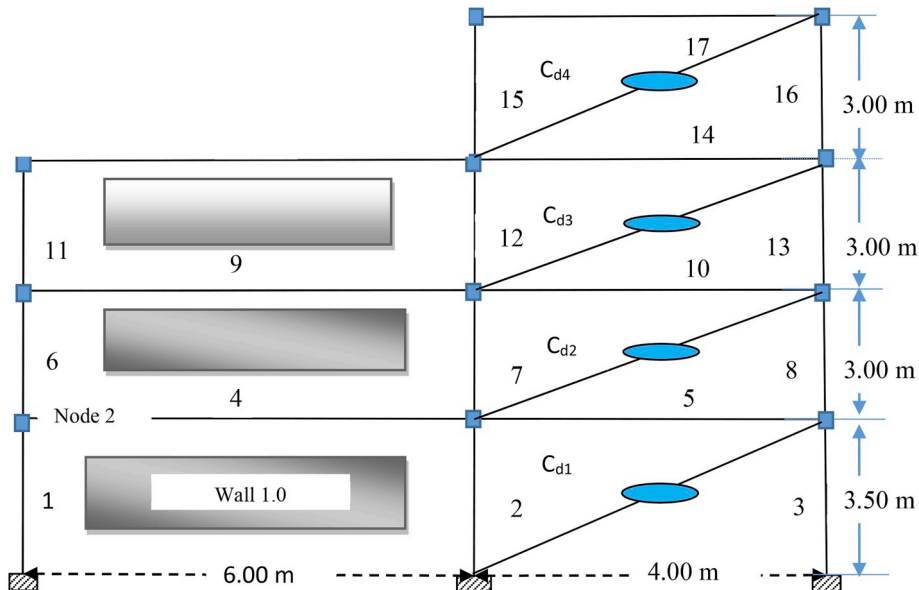


Fig. 3. C_{d_i} refers to added dampers and $i = 1 \dots 4$.

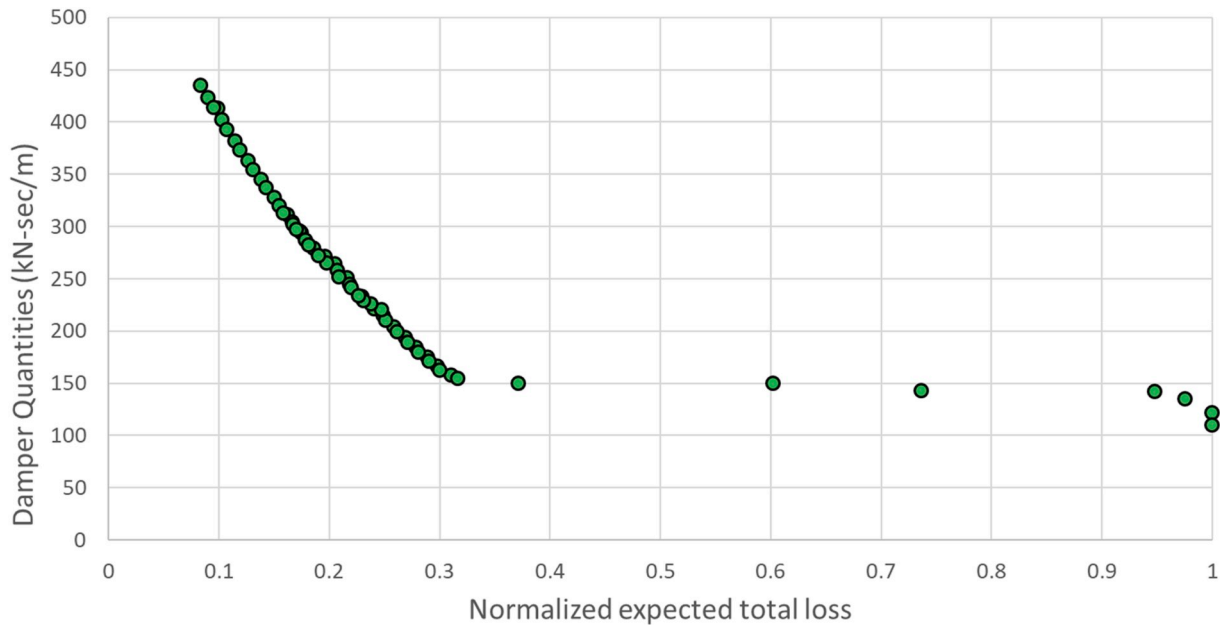


Fig. 4. pareto-front obtained for the four story frame.

partitions) are considered in the present study, this total cost (\$1,163,750) must be scaled down. Adopting the fact that partitions cost $\sim 7.5\%$ and the beam column junction costs $\sim 5.2\%$ of the total cost [72], the total cost gets scaled down to $\sim \$147,797$.

Losses in the partition walls are assumed to be lumped to the nodes of the bay to which the wall is attached by assuming a suitable tributary area. For e.g., for wall 1, 50% of the loss is lumped to node 2 as shown in Fig. 1. The interstorey drift associated with node 2 which is the same for the other nodes at the same level (in the case of node 2, the first floor level) causes the loss in this partition wall. Euler beam elements are used for the modelling of the frame. Elemental Wilson Penzien model is adopted to represent the inherent damping matrix. For more details on implementation of Elemental Wilson Penzien damping model, please refer to Puthanpurayil et al. [68].

A suite of 7 artificial ground motions scaled to match an EC8 design spectra with PGA 0.5 g is used for the present study. Fig. 6 shows the acceleration spectra of ground motions used. As the sole purpose of this study is to illustrate the efficacy of the proposed framework, the artificial suite of ground motions was deemed to be acceptable. It must be mentioned that the framework is very generic and cater to any number of ground motions; as the purpose of this example is just to demonstrate the framework, only 7 ground motions are used. Un-controlled frame analysis has revealed that some of the ground motions scaled to this level of intensity may incur inelastic excursions in the parent frame due to drifts greater than the order of about 1.3% [67]. As already mentioned in section 2.4, it has been observed in the public response to the

Christchurch/Kaikoura sequence of earthquakes that when the building tends to yield or enter inelastic state, the buildings had to be demolished either due to the tendency of owners to claim insurance to build new ones or due to inaccessibility to repair them. So, an effective damper based scheme should incur minimum yielding state in the parent structure. To achieve this objective in the present study, the capping drift d_{al} is limited to 0.8% so that the parent frame is predominantly linear. Only drift sensitive loss is accounted in the present study. Multi-objective optimization is performed as per the methodology described in section 3.0. For the present study only 40 design points are generated in the objective space, i.e. $K = 40$ in step 2 and $q = 4$ as there are only 4 dampers. Constraint *move limit* as required by eq. (16) is adopted as 5% of the design damping vector.

Fig. 4 shows the final Pareto front plotted between initial cost (damper quantities) and the normalized loss. Each of this point on the Pareto front corresponds to a specific quantity of dampers and its distribution. The uncontrolled frame results in a 100% loss as illustrated in Fig. 4 mainly because the drift generated exceeds d_{al} (which is 0.8% for the present example) in at least one of the ground motion.

The Pareto front shown in Fig. 4 illustrates a clear trade-off for the choice of the expected loss and the initial cost. Each point on the Pareto front corresponds to a solution which is obtained by the degraded performance of one of the objectives. For e.g., a point on the extreme right on the x-axis presents a solution where there is a very high loss with minimum initial cost; similarly a point to the left on the x axis shows a minimum loss scenario but with a very high initial cost. So, a whole sphere of possible solutions is represented by the Pareto front and enables the decision maker to quantitatively weigh the trade-offs; i.e. whether to favour one objective in the expense of a degraded performance of the other. Also, in the Pareto front obtained, it could also be seen that there is a substantial decrease in loss with minimum added damping. To illustrate this further, three points on the Pareto front with corresponding loss as 10%, 20% and 30% are selected. The respective quantity of dampers are $402 \text{ kN} - \text{sec}/\text{m}$, $252 \text{ kN} - \text{sec}/\text{m}$ and $154 \text{ kN} - \text{sec}/\text{m}$. The 10% loss corresponds to \$14,779, 20% loss corresponds to \$29,559 and 30% corresponds to \$44,339. It could be clearly seen that to approximately reduce the loss from 30% to 10%, the amount of damping needs to be increased by 2.6 times whereas an increase of '1.6 times the damping quantity would give us a reduction of loss to 20% from 30%. These sorts of information are really useful for

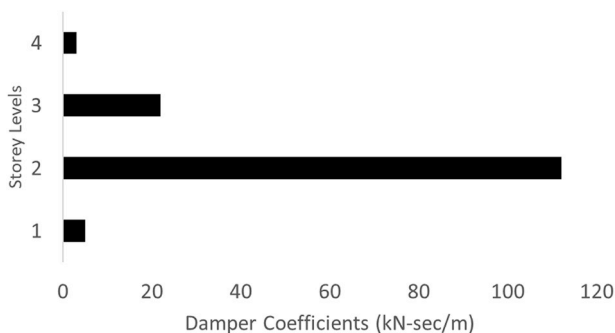


Fig. 5. Optimal distribution of dampers of the selected point in the Pareto front.

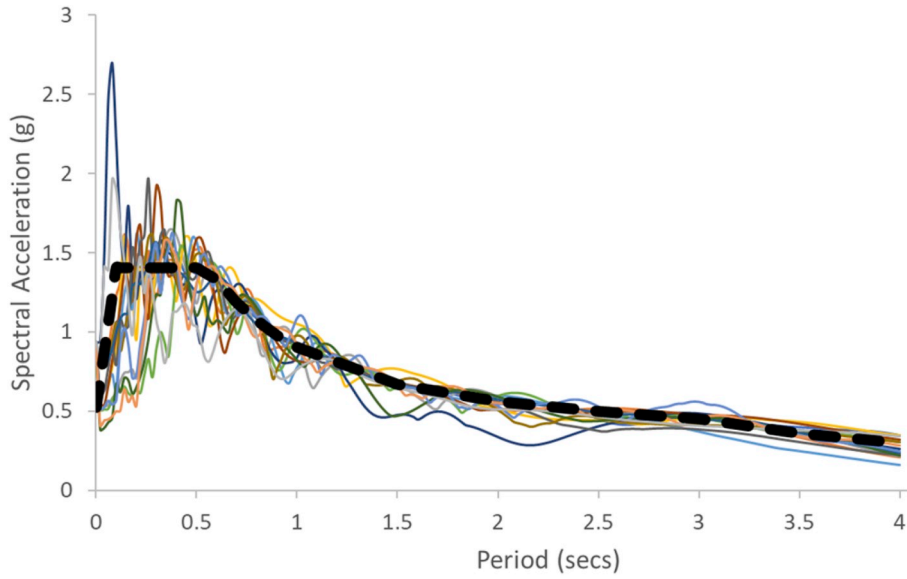


Fig. 6. Acceleration spectra of the scaled ground motions.

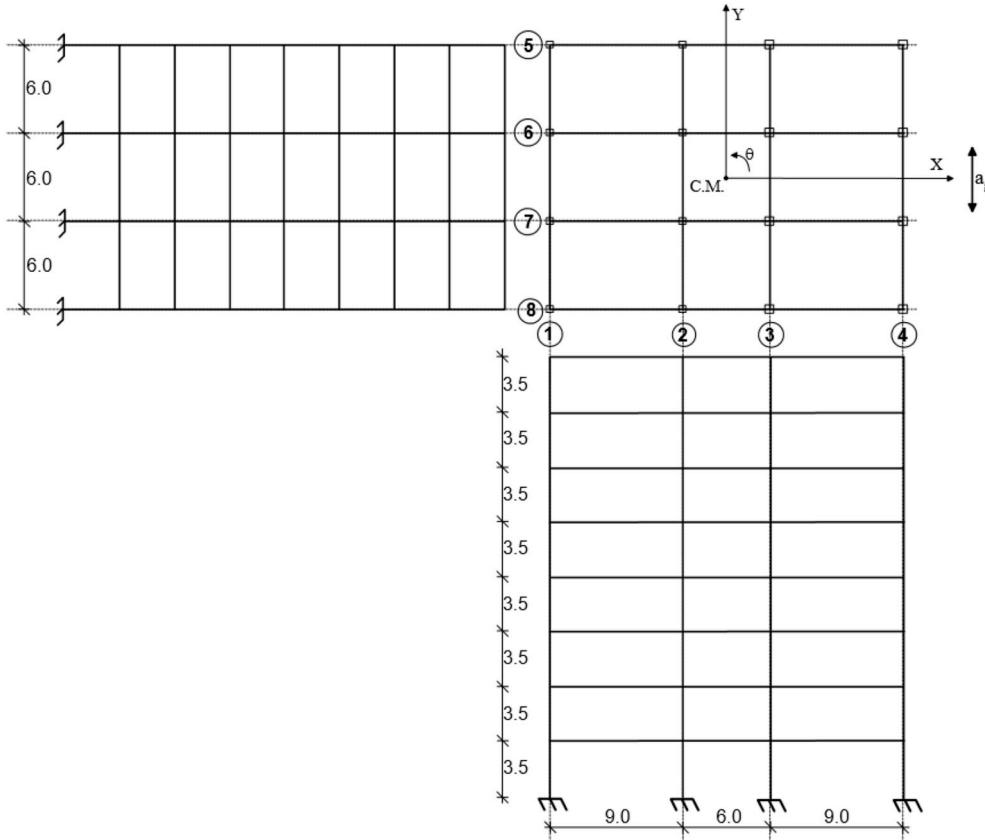


Fig. 7. Eight storey 3 bay by 3 bay RC structure.

Table 3.0
Geometric properties of the structure.

Element location	Beams (width x depth)	Columns (width x depth)
Frames 1 & 4	400 mm × 600 mm	500 mm × 500 mm
Frames 2 & 3	400 mm × 600 mm	700 mm × 700 mm

the stakeholder/owner as he or she can directly see the implications of their choice mainly because the entire front of solutions are available.

The point corresponding to loss of 30% is selected to generate Fig. 5. Damper coefficients are plotted in the horizontal axis and the storey level on the vertical axis. Fig. 5 shows the required quantity of dampers at each level in damper coefficient terms. It may be clearly seen that for a further reduction in loss, a much larger quantity of added damping is required. This quantity corresponds to a first mode damping ratio of approximately 23%. It should be noted that this normalized loss quoted

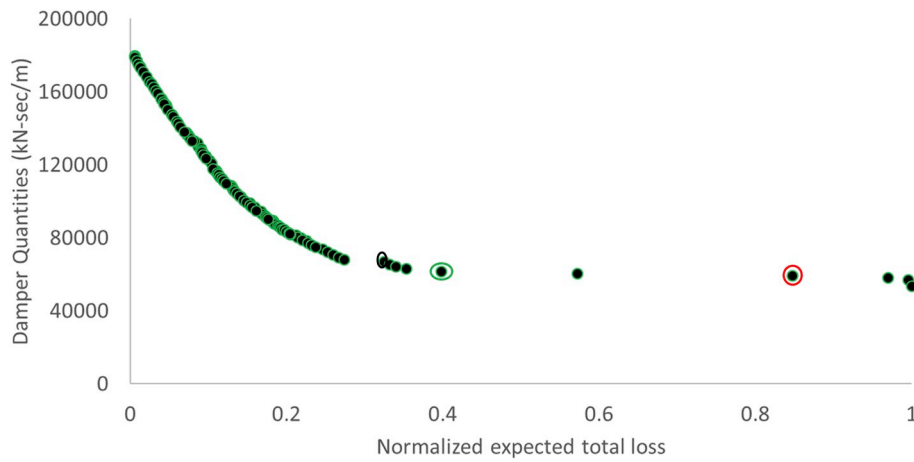


Fig. 8. Pareto front for the 3D structure.

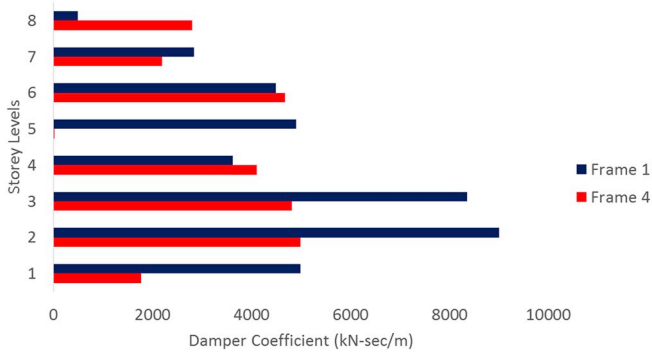


Fig. 9. Viscous damper distribution on the peripheral frames; frame 1 and frame 4.

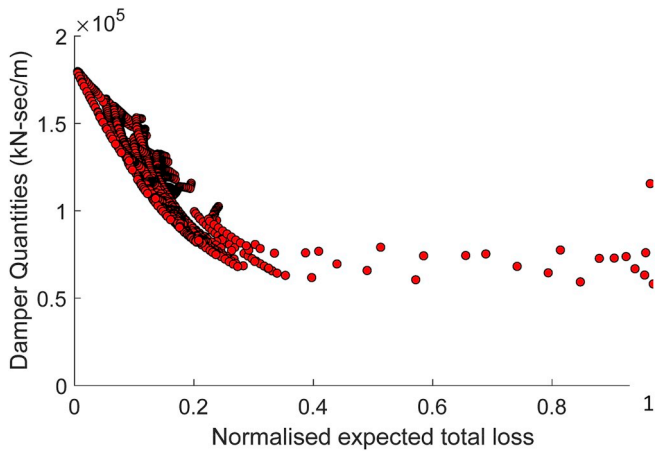


Fig. 10. Migration of the design points to the Pareto front.

is the percentage loss that corresponds to the scaled down total cost (~\$147,797) as described above. So, the approximate loss in dollars comes to ~\$44,339 which is 30% of the scaled down total cost.

4.2. Eight storey 3D asymmetric frame RC structure

An eight storey 3 bay by 3 bay asymmetric framed structure introduced by Tso and Yao [69] and further studied by Lavan and Levy [14] is used for the further study here. Plan and elevations of the structure is shown in Fig. 7.

The geometric properties of the structure are shown in Table 3.0. A uniform floor mass of 0.75 ton/m^2 is uniformly distributed in all

floors. The fundamental period of the system in the y-direction is 1.15 s and, in the x-direction it is 1.225 s.

The modelling of the 3D frame follows the philosophy of assembling the matrix adopted in Wilson and Dovey [73]. Only three degree of freedom is assumed in each floor; The axial deformations are neglected and slab acts as a rigid diaphragm. In majority of the practical structures with in-situ slab construction the assumption of rigid diaphragm may be reasonably justified. Stiffness matrix of each independent frame is assembled first as a plane frame and then the contribution of each of this plane frames to the global 3D frame is computed. More details on this is given in Ref. [14].

Since the present example is only used for demonstrating the applicability of the proposed framework, losses due to structural frame and partitions are only considered in the present study like the previous example. The partition walls are assumed to be distributed uniformly along the height in the outer bays of frame 1 and frame 4. The building is assumed to be in Christchurch, New Zealand and the functionality is categorized as hospitality. As per Rawlinson's pricing manual 2012 [72], a typical cost per floor area is approximately NZ\$ 4750/m². The total floor area is given as 3456 m² which will give an approximate total cost of the building as NZ\$16, 416, 000. This cost includes all components like structure, non-structural, services etc. Since only the structural frame and partitions are considered in the present study, the total cost had to be scaled down to reflect that and it amounts to NZ\$ 2,101,248. This value is called the net considered cost in the present study. This cost is obtained by using the split up that 5.2% of the total cost is attribute to structural frames and 7.5% is attributed to the partitions. Therefore, the obtained Pareto front should be interpreted from this aspect. The losses are lumped at the relevant degrees of freedom and a component-based assessment of loss is adopted as described in section 2.3. To simplify the loss computation, it has been assumed that the distribution of the total cost is the same in all storeys; i.e. if the total cost is "X" and there are "n" storeys, cost per storey is taken as "X/n". In a more realistic case, explicit storey level cost would need to be computed by summing up.

The re-placement value of each of the component comprising the storey. The framework proposed in this study is very generic and can easily incorporate this aspect. Fig. 8 shows the Pareto front. The loss computed is normalized by the net considered cost as described above. Fig. 8 shows the obtained Pareto front. The loss computed is normalized by the net considered cost as described above. For further illustration, let's consider three points as shown in Fig. 8; red circled point corresponds to ~84% loss (NZ\$ 1,765,048) given with a damper quantity of 62.8 MN-sec/m, green circled point refers to ~40% (NZ\$ 840,499) with a total damper quantity of 64.1 MN-sec/m and black circled point refers to a loss of ~30% (NZ\$ 630,374) with a total damper quantity of 67 MN-sec/m. Comparing the red circle and the green circle it is clearly

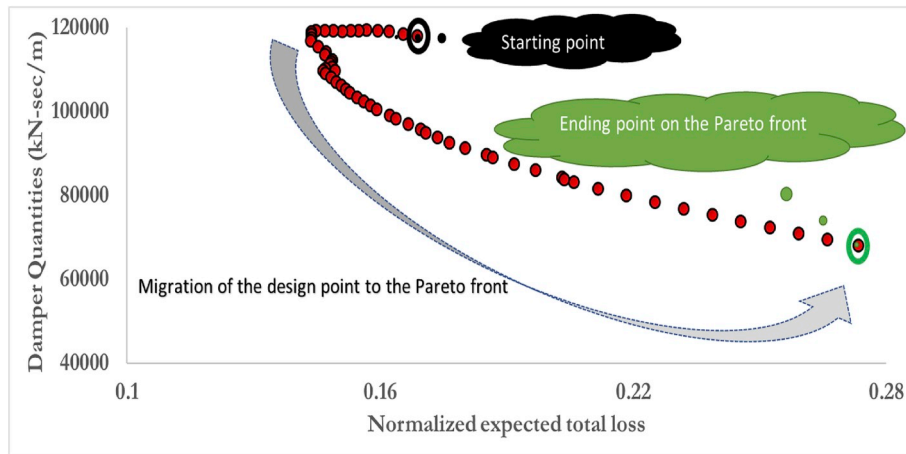


Fig. 11. Migration of the selected design point to the Pareto front as a function of number of iterations.

seen that a reduction in loss of $\sim 52\%$ is obtained by an increase in total damper quantity by $\sim 2\%$; so, basically when we shift from red circled point to green circled point a saving of \sim NZ \$ 924,549 is made; similarly comparing red circle and black circle it may be clearly seen that a reduction by 64% is achieved (saving of NZ \$ 1,134,674) by an increase of just $\sim 7\%$ increase in the damper quantity. This is a very useful information and highlights the benefit of Pareto front emphatically.

Fig. 9 shows a typical viscous damper distribution with a damping ratio of $\sim 40\%$, obtained for the peripheral frames for a typical point identified on the Pareto front of Fig. 8. Although more formal approaches for the computation of the damping ratio have appeared in the literature (e.g. Ref. [70]; or [71]; if a Maxwell model is adopted) the damping ratio here is computed by transforming the damping matrix to the modal coordinates of the undamped structure and neglecting off diagonal elements. Such a computation is common in practice and many researchers and engineers have a feeling to the level of damping achieved using this approach. This point corresponds to a total expected loss of 30% of the net considered cost i.e. a loss of NZ\$ 630,374; now with respect to total structural cost this amounts to 3.8% of total building cost. As described above, only two components (Structural frames and partitions) are considered in this study and this value will increase when more and more components are added. For illustration purpose, this is deemed to be sufficient.

The *controlling* drift which is the d_{cl} in eq. (13) is limited to 0.8% of the story height; this will ensure a predominant elastic response. The presented framework is very generic and can cater to any number of ground motions.

4.2.1. Efficiency of the optimization process

In Fig. 8, only the final Pareto-front is plotted and in Fig. 10, the entire migration of all the design points to the Pareto-front is being depicted. It can be clearly seen that as the iteration progresses, the points migrate to the Pareto front. In Fig. 11 such a migration of one of the design point is being illustrated. The migration of the point to the Pareto-front can be clearly seen from the plot. Starting point and end point have been depicted and the direction of migration is highlighted.

5. Conclusion

In this paper, the design of seismic retrofitting using linear Fluid Viscous Dampers was casted as a multi-objective optimization problem. The objective functions to be minimized are the initial cost of retrofitting and the expected losses. Thus, the Pareto front generated for this problem enables the decision maker, who is typically not an engineer, decide on the level of retrofitting he wishes for based on two competing

objectives he very well understands. Furthermore, his decision could be made with the whole picture at hand showing the trade-off between the investment he makes today in retrofitting the building, to the losses he is expected to suffer in the future.

A first order gradient based optimization scheme is adopted to optimally quantify and distribute the dampers in pre-defined potential locations within the building. Analytical derivation of the first order gradients using the very efficient Adjoint Variable method is presented in detail. This leads to a very computationally efficient approach that can be executed on a personal computer. The approach is applied for the optimal retrofitting of a 2D four storey frame building and a 3D eight storey asymmetric frame building to show the efficiency of the presented scheme and its applicability for the design of retrofitting also for irregular structures.

Acknowledgements

First author gratefully acknowledges the funding provided by Earthquake Commission, New Zealand in the form postgraduate research scholarship.

References

- [1] Puthanpurayil A, Lavan O, Dhakal RP. Multi-Objective loss optimization of seismic retrofitting of moment resisting frames using viscous dampers. 16th World Conference on Earthquake Engineering (16WCEE), Santiago, Chile. 2017.
- [2] Cornell CA, Krawinkler H. Progress and challenges in seismic performance assessment. PEER Cent News 2000;3:1–3.
- [3] Dhakal R, Saha S. Loss optimisation seismic design (LOSD): beyond seismic loss Assessment. Santiago, Chile. 16th world conference on earthquake engineering (16WCEE). 2017. p. 9–13. Jan 2017. : 12.
- [4] Dhakal RP. First step towards loss optimization seismic design (LOSD). Bangkok, Thailand. 3rd asia Conference on Earthquake Engineering (ACEE 2010). 2010. p. 1–3. Dec 2010.
- [5] Christopoulos C, Filiatrault A. Principles of passive supplemental damping and seismic isolation. Iuss press; 2006.
- [6] Constantinou MC, Symans MD. Experimental study of seismic response of buildings with supplemental fluid dampers. Struct Des Tall Special Build 1993;2(issue 2):93–132<https://doi.org/10.1002/tal.4320020203>.
- [7] Dargush GF, Soong TT. Behavior of metallic plate dampers in seismic passive energy dissipation systems. Earthq Spectra 1995;11:545–68<https://doi.org/10.1193/1.1585827>.
- [8] De Domenico D, Ricciardi G, Takewaki I. Design strategies of viscous dampers for seismic protection of building structures: a review. Soil Dyn Earthq Eng 2019;118:144–65.
- [9] Soong TT, Dargush GF. Passive energy dissipation systems in structural engineering. 1997.
- [10] Chakraborty S, Roy R. Seismic behavior of horizontally irregular structures: current wisdom and challenges ahead. Appl Mech Rev 2016;68(6):060802.
- [11] Kawamoto T, Fujita K, Tsuji M, Takewaki I. Robust optimal placement of dampers in structures with set-back and eccentricity using sensitivity analysis for integrated transfer function. Int. J. Earthq. Impact Eng. 2016;1(4):377–94.
- [12] Landi L, Conti F, Diotallevi P. Effectiveness of different distributions of viscous damping coefficients for the seismic retrofit of regular and irregular RC frames. Eng

- Struct 2015;100:79–93.
- [13] Lavan O, Avishur M. Seismic behavior of viscously damped yielding frames under structural and damping uncertainties. *Bull Earthq Eng* 2013;11(6):2309–32.
- [14] Lavan O, Levy R. Optimal peripheral drift control of 3D irregular framed structures using supplemental viscous dampers. *J Earthq Eng* 2006;10(6):903–23.
- [15] Mazza F. Nonlinear seismic analysis of r.c. framed buildings with setbacks retrofitted by damped braces. *Eng Struct* 2016;126:559–70.
- [16] Lavan O, De Stefano M, editors. *Seismic behaviour and design of irregular and complex civil structures*. Dordrecht: Springer; 2013.
- [17] Saatcioglu Murat, Palermo Dan, Ghobarah Ahmed, Mitchell Denis, Simpson Rob, Adebar Perry, Tremblay Robert, Ventura Carlos, Hong Hanping. Performance of reinforced concrete buildings during the 27 February 2010 Maule (Chile) earthquake. *Can J Civ Eng* 2013;40(8):693–710.
- [18] Moehle JP, Alarcon LF. Seismic Analysis methods for irregular buildings. *J Struct Eng* 1986;112:35. (1986)112:1(35). [https://doi.org/10.1061/\(ASCE\)0733-9445](https://doi.org/10.1061/(ASCE)0733-9445).
- [19] Lavan O, Dargush GF. Multi-objective evolutionary seismic design with passive energy dissipation systems. *J Earthq Eng* 2009;13(6):758–90.
- [20] Lavan O. On the efficiency of viscous dampers in reducing the various seismic responses of wall structures. *Earthq Eng Struct Dyn* 2012;41(Issue 12):1673–92 <https://doi.org/10.1002/eqe.1197>.
- [21] Hahn GD, Sathivageeswaran KR. Effects of added-damper distribution on the seismic response of buildings. *Comput Struct* 1992;43(5):941–50.
- [22] Agrawal AK, Yang JN. Design of passive energy dissipation systems based on LQR control methods. *J Intell Mater Syst Struct* 1999;10(12):933–44 <https://doi.org/10.1106/FB58-N1DG-EJCJT-B8H4>.
- [23] Gluck N, Reinhorn AM, Gluck J, Levy R. Design of supplemental dampers for control of structures. *J Struct Eng, ASCE* 1996;122(12):1394–9.
- [24] Lin TK, Hwang JS, Chen KH. Optimal distribution of damping coefficients for viscous dampers in buildings. *Int J Struct Stab Dyn* 2017;17(04):1750054.
- [25] Lopez-Garcia D. A simple method for the design of optimal damper configuration in MDOF structures. *Earthq Spectra* 2001;17(3):38–398.
- [26] Loh CH, Lin PY, Chung NH. Design of dampers for structures based on optimal control theory. *Earthq Eng Struct Dyn* 2000;29(9):1307–23.
- [27] Ribakov Y, Gluck J. Optimal design of ADAS damped MDOF structures. *Earthq Spectra* 1999;15:317–30.
- [28] Ribakov Y, Reinhorn AM. Design of amplified structural damping using optimal considerations. *J Struct Eng* 2003;129(10):1422–7. 2003)129:10(1422). [https://doi.org/10.1061/\(ASCE\)0733-9445](https://doi.org/10.1061/(ASCE)0733-9445).
- [29] Shukla AK, Datta TK. Optimal use of viscoelastic dampers in building frames for seismic force. *J Struct Eng, ASCE* 1999;125(4):401–9.
- [30] Wongprasert N, Symans MD. Application of a genetic algorithm for optimal damper distribution within the nonlinear seismic benchmark building. *J Eng Mech* 2004;130:4:401–6.
- [31] Xu YL, Teng J. Optimum design of active/passive control devices for tall buildings under earthquake excitation. *Struct Des Tall Build* 2002;11(2):109–27.
- [32] Yang G, Spencer Jr. BF, Carlson JD, Sain MK. Large-scale MR fluid dampers: modeling and dynamic performance considerations. *Eng Struct* 2002;24(3):309–23.
- [33] Zhang RH, Soong TT. Seismic design of visco-elastic dampers for structural applications. *J Struct Eng* 1992;118(5):1375–92.
- [34] Agrawal AK, Yang JN. Optimal placement of passive dampers on seismic and wind excited buildings using combinatorial optimization. *J Intell Mater Syst Struct* 1999;10(12):997–1014 <https://doi.org/10.1106/YV3B-TP5H-HWQ2-X1OK>.
- [35] Constantinou MC, Tadjabakhsh IG. Optimum design of a first story damping system. *Comput Struct* 1983;17(2):305–10.
- [36] Singh MP, Moreschi LM. Optimal seismic response control with dampers. *Earthq Struct Dyn*. 2001;30(4):553–72.
- [37] Singh MP, Moreschi LM. Optimal placement of dampers for passive response control. *Earthq Struct Dyn*. 2002;31(4):955–76.
- [38] Takewaki I. Optimal damper placements for minimum transfer functions. *Earthq Eng Struct Dyn* 1997;26(11):1113–24.
- [39] Takewaki I. Efficient redesign of damped structural systems for target transfer functions. *Comput Methods Appl Mech Eng* 1997;147(3–4):275–86.
- [40] Almazán JL, de la Llera JC. Torsional balance as new design criterion for asymmetric structures with energy dissipation devices. *Earthq Eng Struct Dyn* 2009;38(12):1421–40.
- [41] Aydin E, Boduroglu MH, Guney D. Optimal Dampers Placements for Seismic rehabilitation of planar building structures. *Eng Struct* 2007;29:176–85.
- [42] Cetin H, Aydin E, Ozturk B. Optimal damper allocation in shear buildings with tuned mass dampers and viscous dampers. *Int. J. Earthq. Impact Eng.* 2017;2(2):89–120.
- [43] Dargush GF, Sant RS. Evolutionary aseismic design and retrofit structures with passive energy dissipation. *Earthq Eng Struct Dyn* 2005;34:1601–26 <https://doi.org/10.1002/eqe.497>.
- [44] Huang X. Evaluation of genetic algorithms for the optimum distribution of viscous dampers in steel frames under strong earthquakes. *Earthq. Struct.* 2018;14(3):215–27.
- [45] Lavan O, Levy R. Optimal design of supplemental viscous dampers for linear framed structures. *Earthq Eng Struct Dyn* 2006;35(3):337–56.
- [46] Levy R, Lavan O. Fully stressed design of passive controllers in framed structures for seismic loadings. *Struct Multidiscip Optim* 2006;32(6):485–98.
- [47] Liu W, Tong M, Lee GC. Optimization methodology for damper configuration based on building performance indices. *J Struct Eng* 2005;131(11):1746–56.
- [48] Park JH, Kim J, Min KW. Optimal design of added viscoelastic dampers and supporting braces. *Earthq Eng Struct Dyn* 2004;33(4):465–84.
- [49] Wang S, Mahin SA. High-performance computer-aided optimization of viscous dampers for improving the seismic performance of a tall building. *Soil Dyn Earthq Eng* 2018;113:454–61.
- [50] Xie Y, Zhang J, Xi W. Effectiveness evaluation and optimal design of nonlinear viscous dampers for inelastic structures under pulse-type ground motions. *Earthq Eng Struct Dyn* 2018;47(14):2802–20.
- [51] Zare AR, Ahmadzadeh M. Design of passive viscous fluid control systems for nonlinear structures based on active control. *J Earthq Eng* 2017:1–22.
- [52] Gidarisi I, Taflanidis AA. Performance assessment and optimization of fluid viscous dampers through life-cycle cost criteria and comparison to alternative design approaches. *Bull Earthq Eng* 2015;13(4):1003–28.
- [53] Shin H, Singh MP. Minimum failure cost-based energy dissipation system designs for buildings in three seismic regions – Part II: application to viscous dampers. *Eng Struct* 2014;74:275–82.
- [54] Altieri D, Tubaldi E, De Angelis M, Patelli E, Dall'Asta A. Reliability-based optimal design of nonlinear viscous dampers for the seismic protection of structural systems. *Bull Earthq Eng* 2018;16(2):963–82.
- [55] Pareto V. *Manuel d'économie Politique*, Giard, Paris. 1927.
- [56] Lavan O, Amir O. Simultaneous topology and sizing optimization of viscous dampers in seismic retrofitting of 3D irregular frame structures. *Earthq Eng Struct Dyn* 2014;43(9):1325–42.
- [57] Pollini N, Lavan O, Amir O. Minimum-cost optimization of nonlinear fluid viscous dampers and their supporting members for seismic retrofitting. *Earthq Eng Struct Dyn* 2017;46(12):1941–61.
- [58] Pollini N, Lavan O, Amir O. Towards realistic minimum-cost optimization of viscous fluid dampers for seismic retrofitting. *Bull Earthq Eng* 2016;14(3):971–98.
- [59] Pollini N, Lavan O, Amir O. Optimization-based minimum-cost seismic retrofitting of hysteretic frames with nonlinear fluid viscous dampers. *Earthq Eng Struct Dyn* 2018;47(15):2985–3005.
- [60] Bahnasy A, Lavan O. Linear or nonlinear fluid viscous dampers? A seismic point of view. *Structures congress 2013: bridging your passion with your profession*. 2013. p. 2253–64.
- [61] Tubaldi E, Ragni L, Dall'Asta A. Probabilistic seismic response assessment of linear systems equipped with nonlinear viscous dampers. *Earthq Eng Struct Dyn* 2015;44(1):101–20.
- [62] Miyamoto HK, Gilani AS, Wada A, Ariyaratana C. Limit states and failure mechanisms of viscous dampers and the implications for large earthquakes. *Earthq Eng Struct Dyn* 2010;39(11):1279–97.
- [63] Aslani H, Miranda E. Probabilistic earthquake loss estimation and loss disaggregation in buildings. *Univ. Stanf.* 2005:66–219. Research report No:15.
- [64] Ramirez MC, Miranda E. Building-Specific loss estimation methods & tools for simplified performance-based earthquake engineering Stanford University; 2009. Report No:171.
- [65] Izui K, Yamada T, Nishiwaki S, Tanaka K. Multiobjective optimization using an aggregative gradient-based method. *Struct Multidiscip Optim* 2015;51(1):173–82.
- [66] Lavan O. Multi-objective optimal design of tuned mass dampers. *Struct Control Health Monit* 2017;24(11):e2008.
- [67] Arede AJCD. Seismic assessment of reinforced concrete frame structures with a new flexibility based element Research Thesis Univ. do Porto 1997:191–336.
- [68] Puthanpurayil AM, Lavan O, Carr AJ, Dhakal RP. Elemental damping formulation: an alternative modelling of inherent damping in nonlinear dynamic analysis. *Bull Earthq Eng* 2016;14:2405–34.
- [69] Tso WK, Yao S. Seismic load distribution in buildings with eccentric setback. *Can J Civ Eng* 1994;21(1):50–62.
- [70] Hurty WC, Rubinstein MF. *Dynamics of structures*. Prentice-Hall series in engineering of the physical sciences. Englewood Cliffs: Prentice-Hall; 1964.
- [71] Zambrano A, Inaudi JA, Kelly JM. Modal coupling and accuracy of modal strain energy method. *J Eng Mech* 1996;122(7):603–12.
- [72] Rawlinsons *New Zealand construction handbook* (2012).
- [73] Wilson EL, Dovesy HH. Three dimensional analysis of building systems-TABS Earthquake Engineering Research Center. College of Engineering, University of California; 1972. Report (University of California, Berkeley. Earthquake Engineering Research Center), no. EERC 72-8.
- [74] Jensen SJ, Nakshtathala PB, Tortorelli DA. On the consistency of adjoint sensitivity analysis for structural optimization of linear dynamic problems. *Structural and Multidisciplinary Optimization* 2013;49(5):831–7.